

Dynamical design of spatial patterns of colloidal suspensions

N. A. M. Araújo,^{1,*} D. A. Zezyulin,^{2,3,1,†} V. V. Konotop,^{1,‡} and M. M. Telo da Gama^{1,§}

¹*Departamento de Física, Faculdade de Ciências,
Universidade de Lisboa, P-1749-016 Lisboa, Portugal,
and Centro de Física Teórica e Computacional, Universidade de Lisboa,
Avenida Professor Gama Pinto 2, P-1649-003 Lisboa, Portugal*

²*ITMO University, St. Petersburg 197101, Russia*

³*Institute of Mathematics with Computer Center, Ufa Scientific Center,
Russian Academy of Sciences, Chernyshevskii str., 112, Ufa 450008, Russia*

We study the collective dynamics of colloidal suspensions in the presence of a time-dependent potential, by means of dynamical density functional theory. We consider a non-linear diffusion equation for the density and show that spatial patterns emerge from a sinusoidal external potential with a time-dependent wavelength. These patterns are characterized by a sinusoidal density with the average wavelength and a Bessel-function envelope with an induced wavelength that depends only on the amplitude of the temporal oscillations. As a generalization of this result, we propose a design strategy to obtain a family of spatial patterns using time-dependent potentials of practically arbitrary shape.

I. INTRODUCTION

The emergence of spatio-temporal patterns in systems driven away from equilibrium has been always intriguing for scientists and laymen alike [1, 2]. Understanding how collective patterns emerge from the local interactions is not only a question of scientific curiosity, but also of technological interest, for the resulting patterns are related in a non-trivial way to the physical properties of the system.

Colloidal suspensions are an example of such systems. With a typical size of the order of the micron, individual colloidal particles are characterized by Brownian motion, in very dilute suspensions. However, as the density increases, correlations among these random walkers lead to their spontaneous self-organization into mesoscopic structures that extend over length scales that are much larger than the typical range of the particle-particle interactions [3–6].

Several strategies have been explored to control self-organization to drive it towards desired structures including, for example, the fine tuning of the particle-particle interactions [7–9], the control of the suspending medium [10], and the presence of external constraints such as: interfaces [11, 12], substrates [9, 13–16], or electromagnetic fields [17–28]. In this paper, we will consider the case of electromagnetic fields. They not only help to control the rotational degrees of freedom [23] or fine tune the particle-particle interactions [21, 22, 24], but they can also act as virtual molds to induce spatial periodic patterns [25–27], as we discuss below.

The time evolution of the system will be described using dynamic density functional theory [29, 30]. Assuming an adiabatic evolution, it is possible to write down a

non-linear diffusion equation for the local density, from the equilibrium Helmholtz free energy functional. Such a coarse-grained description still grasps several relevant non-equilibrium properties and allows accessing the relevant time and length scales of pattern formation [31, 32].

The paper is organized in the following way. The model and the methods are discussed in the next section. Results are presented and discussed in Sec. III. Final remarks are made in Sec. IV.

II. MODEL AND METHODS

Let us consider a system of colloidal particles in the overdamped regime. The interaction between two particles is described by a purely-repulsive pairwise potential $V(r)$, where r is the distance between particle centers. The potential associated to the external field V_{ext} is assumed periodic (sine function) along the x -direction. For stationary periodic potentials, particles tend to accumulate along the minima of the potential forming bands along the y -direction [33]. In order to study the effect of time-dependent potentials, we consider that the characteristic wavelength of the external field creating the spatial lattice oscillates periodically in time around unity. Thus the particle-field interaction is described by the potential,

$$V_{\text{ext}}(\vec{r}, t) = V_0 \sin([1 - V_1 \sin(\omega t)] x) , \quad (1)$$

where ω is a frequency and t is the time in units of the Brownian time $\tau_B = r_p^2 \gamma (k_B T)^{-1}$ (the time over which a colloidal particle diffuses over a region equivalent to r_p^2), where r_p is the radius of the colloidal particles, k_B is the Boltzmann constant, T is the temperature, and γ the Stokes coefficient. V_0 and V_1 are the amplitudes of the potential and oscillations, respectively. In the limit $V_1 = 0$, the stationary potential with unit wavelength is recovered, setting the units of length, while for $V_0 = 0$,

* nmaraujo@fc.ul.pt

† dzezyulin@fc.ul.pt

‡ vvkonotop@fc.ul.pt

§ mmgama@fc.ul.pt

purely-repulsive particles are expected to be distributed uniformly in space.

The Helmholtz free energy functional of the system can be approximated as [29],

$$\begin{aligned} \mathcal{F}[\rho(\vec{r}, t)] &= k_B T \int \rho(\vec{r}, t) [\log(\rho(\vec{r}, t)\Lambda^2) - 1] d\vec{r} \\ &+ \frac{1}{2} \int \int \rho(\vec{r}, t)\rho(\vec{r}', t)V(|\vec{r} - \vec{r}'|)d\vec{r}'d\vec{r} \\ &+ \int \rho(\vec{r}, t)V_{\text{ext}}(\vec{r}, t)d\vec{r} \ , \end{aligned} \quad (2)$$

where, Λ is the thermal de Broglie wavelength (with units of length) and $\rho(\vec{r}, t)$ is the (number) density, defined as the number of colloidal particles per unit area, in two dimensions. The first term is the free energy of the ideal gas, the second term corresponds to a mean-field approximation of the pairwise correlations, and the third one is the interaction with the external field.

From the dynamic density-functional theory (DDFT), assuming adiabatic evolution of the system, one can obtain the time evolution of the density from the equilibrium Helmholtz free energy functional [29],

$$\gamma \frac{\partial \rho(\vec{r}, t)}{\partial t} = \nabla \left[\rho(\vec{r}, t) \nabla \frac{\delta \mathcal{F}[\rho(\vec{r}, t)]}{\delta \rho(\vec{r}, t)} \right]. \quad (3)$$

Assuming the local density approximation (LDA) [33], $\rho(\vec{r}', t) \approx \rho(\vec{r}, t) + (\vec{r}' - \vec{r}) \nabla \rho$, and the functional defined in Eq. (2), one can obtain a non-linear diffusion equation for the time evolution of the density,

$$\gamma \frac{\partial \rho}{\partial t} = \nabla \left[A \rho \nabla \rho + \frac{\partial V_{\text{ext}}}{\partial x} \rho \mathbf{i} \right] + k_B T \Delta \rho \ . \quad (4)$$

Here, \mathbf{i} is the unit vector directed along the x -axis, and $A = \int V(\vec{r}') d\vec{r}'$, where the integral is over the entire space, is a positive constant for a purely-repulsive pairwise interaction [33]. The first two terms are related to the particle-particle and particle-field interactions, while the third one results from the interaction with the suspending medium.

III. RESULTS

Given the translational invariance of $V_{\text{ext}}(\vec{r}, t)$ along the y -direction (see Eq. (1)), we solve numerically a 1D version of Eq. (4) in a finite domain, with periodic boundary conditions, to reduce finite-size effects. The domain size is such that $x \in [-400, 400]$ in length units; numerical results for a smaller domain $x \in [-200, 200]$ revealed no significant dependence on the domain size. Without loss of generality, we consider $\gamma = 1$ and $k_B T = 1$, which can be mapped to any other values by properly rescaling x and t , in Eq. (4). $k_B T = 1$ sets the energy scale, such that V_0 is defined in units of $k_B T$. Rescaling the mean density, one can also assume that $A \in \{\pm 1, 0\}$. As initial conditions, we considered a uniform density profile

($\rho_0 = 1/(2\pi)$). Tests with different initial conditions, but the same average density, revealed no dependence of the final pattern on the initial conditions.

As summarized in Fig. 1, spatio-temporal patterns are obtained in the presence of the time-dependent field. While for slow variations of the wavelength of the potential (low ω), the density follows the time evolution of the potential (Figs. 1(a)-(c)), for sufficiently rapid variations (high ω), a spatial pattern emerges with a stationary envelope and a non-stationary filling, that persists over time (Fig. 1(d)). However, the characteristic wavelength of the emerging pattern does not seem to depend on the value of ω . We also observe dynamical localization at the center of the box, which is not observed in the stationary case ($V_1 = 0$). This is a consequence of the shape of the potential (1), since at $x = 0$ the value of the potential does not change with time.

A. Effect of the averaged potential

The appearance of a new spatial scale in a time-varying potential can be understood using averaging arguments. At high enough ω , we assume that the temporal dependence of the density is much slower than the variation of the potential. Then, the density can be considered approximately constant during one period of the potential oscillation, i.e., in the interval $(t, t + 2\pi/\omega)$, $\omega \gg 1$. Performing the average over one period (i.e., multiplying by $2\pi/\omega$ and integrating from $t = \tau$ to $t = \tau + 2\pi/\omega$), we conclude that the rapidly oscillating potential can be approximated by an effective averaged potential:

$$\langle V(x) \rangle = \frac{\omega}{2\pi} \int_0^{2\pi/\omega} V_{\text{ext}}(x, t) dt. \quad (5)$$

Thus, instead of Eq. (4), we consider

$$\frac{\partial \rho}{\partial t} = \nabla \left[A \rho \nabla \rho + \frac{d\langle V(x) \rangle}{dx} \rho \mathbf{i} \right] + \Delta \rho, \quad (6)$$

where, according to the above discussion, we rescaled γ and $k_B T$ to unity. To obtain a time-independent solution, we solve the 1D version of this equation,

$$[A \rho_x \rho + \langle V(x) \rangle_x \rho]_x + \rho_{xx} = 0, \quad (7)$$

where ρ_x and ρ_{xx} are the first and second spatial derivatives along the x -direction, respectively. This equation can be integrated, which gives $A \rho_x \rho + \langle V(x) \rangle_x \rho + \rho_x = C_0$, where C_0 is some constant. We set $C_0 = 0$, corresponding to $\rho_x = 0$ when $\rho = 0$, and we integrate the resulting equation again, which gives

$$A \rho + \ln \rho = -\langle V \rangle + C_1. \quad (8)$$

For the particular choice (1), we find

$$\langle V \rangle = V_0 \sin(x) J_0(V_1 x), \quad (9)$$

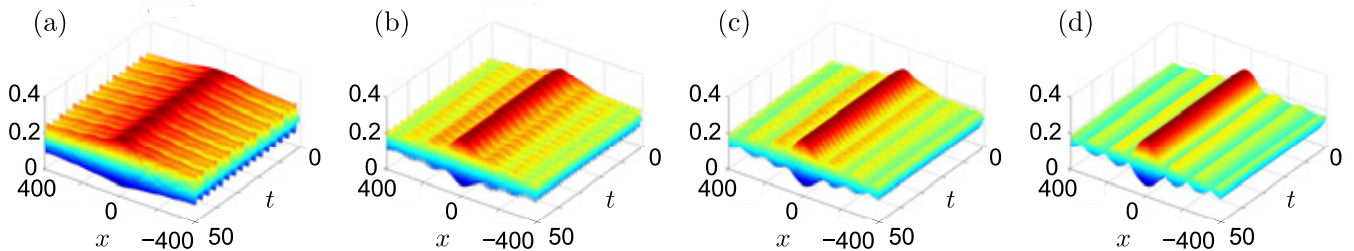


FIG. 1. Time evolution of the density profile $\rho(x, t)$, for a 1D system with $V_1 = 0.025$, and different values of ω , namely: (a) 1, (b) 2, (c) 3, and (d) 10. The results were obtained by solving Eq. (4) numerically, in a domain with size 800 and periodic boundary conditions. Asymptotically, a spatially varying pattern emerges with a characteristic wavelength that decreases with V_1 .

where J_0 is the zero-order Bessel function. Thus, if $V_1 \ll 1$, as in Fig. 1, the average potential consists of the product of a rapidly oscillating $\sin(x)$ and a slowly varying envelope $J_0(V_1 x)$. The latter can be used to compute the smooth envelope of the density ρ_s :

$$A\rho_s + \ln \rho_s = -V_0 J_0(V_1 x) + C_2. \quad (10)$$

When $A = 0$ this equation admits a simple analytical solution; for nonzero A it has to be solved numerically. The constant C_2 is determined from the value of the mean density. Thus the slow spatial scale is described by the oscillating zero-order Bessel function $J_0(V_1 x)$. At large $|x|$, the distance between the successive zeros of $J_0(x)$ approaches π . Thus the distance between the “nodes” of the pattern ρ_s can be estimated as π/V_1 , which is in good agreement with the numerical results.

In order to make a simple check, we consider $A = 0$ in Eq. (10) and obtain

$$\rho_s = B \exp[-V_0 J_0(V_1 x)], \quad (11)$$

where $B = \exp(C_2)$. Thus, the slow envelope is proportional to $\exp[-V_0 J_0(V_1 x)]$, in agreement with the observed pattern, see Fig. 2. For nonzero A , Eq. (8) is solved numerically (see Fig. 3 and the example for $A = 1$, in the next section).

B. Designing spatial patterns

In the previous section, we have shown that a spatial pattern emerges from the interaction with a time-dependent potential. We now develop a framework to reverse-engineer the pattern and determine the external potential that leads to a given pattern. To do so, let us first show how to use a combination of sine potentials with time-dependent wavelengths to obtain an effective average potential with a slow cosine-shaped envelope.

Let us consider a potential in the form of the superposition $V_{ext} = \sum_{n=0}^{\infty} V_n$, where a $2\pi/\omega$ -periodic (in time)

elementary block reads

$$V_n = V_0^{(n)} \sin\left(\left[1 - V_1^{(n)} \sin(\omega t)\right] x + 2n\omega t\right), \quad (12)$$

$n = 0, 1, \dots$

Notice that Eq. (1) was generalized by adding a time-dependent spatial shift $2n\omega t$, i.e., now in the expansion over the propagation, non-stationary waves are used. The average of the n th elementary block reads

$$\langle V_n \rangle = V_0^{(n)} \sin(x) J_{2n}(V_1^{(n)} x), \quad (13)$$

where J_{2n} is the $2n$ th Bessel function. Thus the average of the superposition has the form

$$\langle V \rangle = \sin(x) \sum_{n=0}^{\infty} V_0^{(n)} J_{2n}(V_1^{(n)} x) \quad (14)$$

and the density profile is given by Eq. (8).

We now consider an example of another average potential that can be dynamically engineered. To this end, we use the expansion of the cosine function on Bessel functions,

$$\cos z = J_0(z) - 2J_2(z) + 2J_4(z) - 2J_6(z) + \dots \quad (15)$$

Thus, for $V_1^{(1)} = V_1^{(2)} = \dots = V_1$, $V_0^{(0)} = 1$, $V_0^{(1)} = V_0^{(3)} = V_0^{(5)} = \dots = -2$, and $V_0^{(2)} = V_0^{(4)} = V_0^{(6)} = \dots = 2$, the average potential is

$$\langle V \rangle = \sin(x) \cos(V_1 x). \quad (16)$$

For small V_1 , the average potential has the structure of the slow envelope $\cos(V_1 x)$ and fast filling $\sin(x)$. Omitting the latter contribution, using Eq. (8) we obtain for the smooth envelope ρ_s of the density

$$A\rho_s + \ln \rho_s = -V_0 \cos(V_1 x) + C_4, \quad (17)$$

where C_4 is a constant. When $A = 0$, this equation admits a simple analytical solution; for nonzero A it should be solved numerically. Recall that the constant on the right-hand side is obtained from the value of the mean

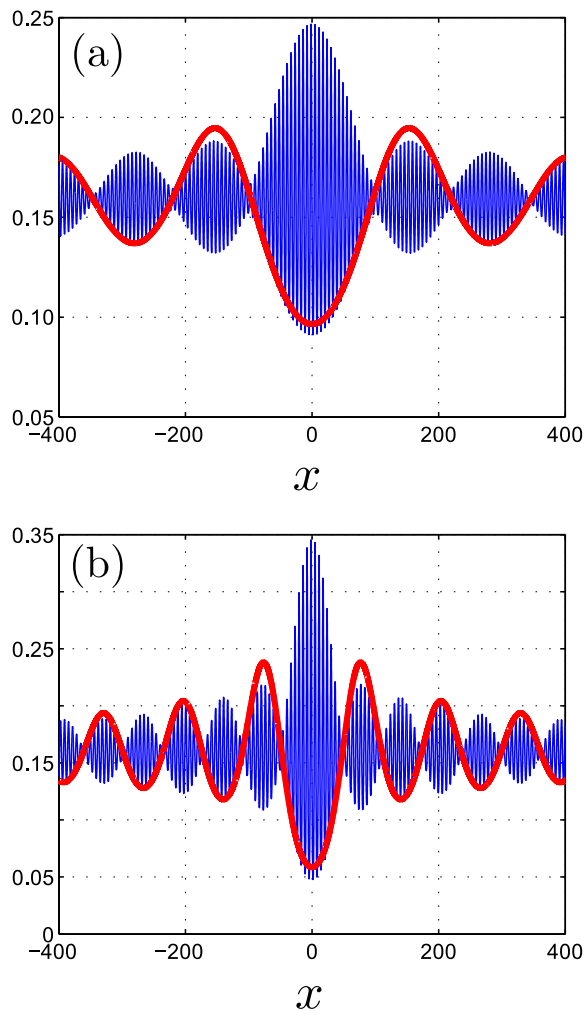


FIG. 2. Density, $\rho(x)$, at $t = 0$, for a 1D system. The blue curve was obtained by solving Eq. (4), in a domain with size 800 unit lengths and periodic boundary conditions, for $A = 0$, (a) $V_0 = 0.5$, $V_1 = 0.025$ and (b) $V_0 = 1$, $V_1 = 0.05$. The red curves are given by $B \exp[-V_0 J_0(V_1 x)]$, where B was adjusted to fit the numerical data.

density. In practice, the expansion (15) is truncated at a finite number of terms, and therefore the resulting averaged potential will be affected by the truncation. Figure 3 depicts the numerical results for eight terms in the expansion (15). The resulting pattern (blue line in Fig. 3(b)) is compatible with the envelope ρ_s , estimated from Eq. (17), corresponding to the red line.

Even more generally, normalizing the interval along the x-axis to $[0, 1]$, one can use the fact that the Bessel functions form a complete set, i.e., on a given interval $[0, 1]$, the Bessel functions $\sqrt{x} J_n(V_k^{(n)} x)$, constitute a complete set, and thus any functional dependence of the envelope on the average potential ($\langle V \rangle(x)$) can be expanded in Bessel functions. Thus, with a proper parameterization of the potential given by Eq. (12), one can

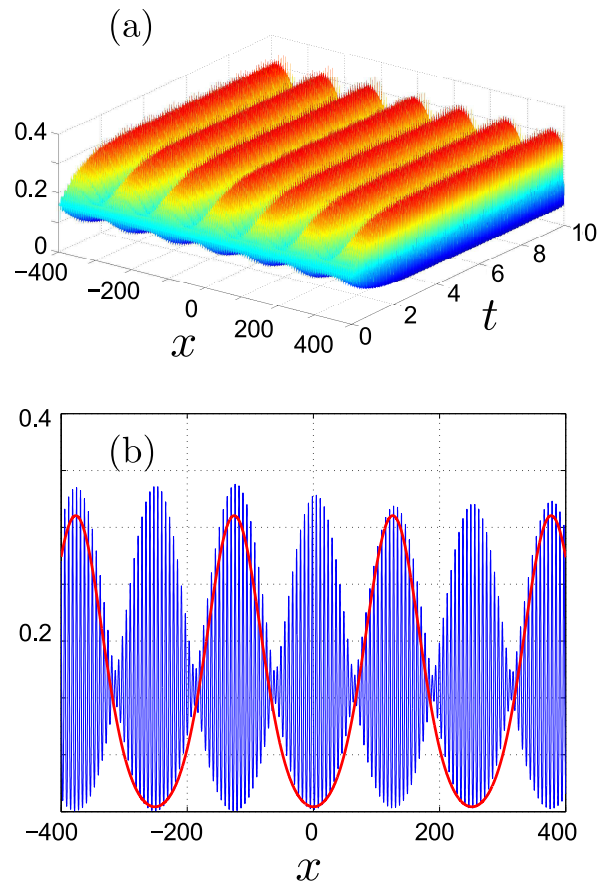


FIG. 3. (a) Time evolution of the density profile $\rho(x, t)$, obtained by solving Eq. 8 in a 1D domain with 800 unit lengths and periodic boundary conditions. V_{ext} corresponds to a cosine-shaped potential, obtained from Eq. (14), truncated after eight terms. (b) Comparison of the density profile $\rho(x)$, at $t = 10$ (blue curve), with the slow envelope ρ_s (red curve) found numerically from Eq. (17). The other parameters are $A = 1$, $\omega = 20$, and $V_1 = 0.025$.

obtain the targeted envelope.

In short, to obtain a given periodic pattern, one needs to invert Eq. (8) to compute the average potential $\langle V(x) \rangle$, which supports the given pattern. Then, the average potential is expanded in terms of Bessel functions (or Fourier series over cosines) and the potential in Eq. (12) is parameterized accordingly.

IV. FINAL REMARKS

We have studied the collective dynamics of colloidal suspensions in the presence of time-varying potentials. Using dynamic density-functional theory, the local interactions can be coarse-grained to obtain a non-linear diffusion equation for the time evolution of the density, allowing us to access the relevant time and length scales to observe the formation of spatio-temporal patterns. For

a potential with sinusoidal spatial symmetry and a characteristic wavelength that varies periodically with time, we have shown that a spatial pattern emerges, at high enough frequencies, with a stationary envelope. However, the new characteristic length, does not seem to depend on the frequency of oscillations but rather on their amplitude. Using averaging arguments, we obtained an equation for the envelope of the pattern and its dependence on the amplitude of the oscillations. This equation is in good agreement with the patterns obtained by numerical solution of the non-linear diffusion equation. The patterns described here resemble Faraday patterns, which typically appear in vibrating recipients. Different from those patterns, here it is the wavelength of the external field that oscillates rather than the magnitude of the field.

After establishing the relationship between the potential and the properties of the emerging pattern, it was possible to develop a reverse engineering strategy to tune the pattern by changing the amplitude and frequency of the potential oscillations. Any pattern envelope that can be expanded over a series of Bessel functions can be obtained with this method. To access the relevant time and length scales, we have considered a coarse-grained (continuum) description of the colloidal suspension, assuming that the size of the colloidal particles is much

smaller than the other length scales. For values of the average wavelength comparable to the particle size, one expects that the discrete nature of the particles plays a role, and other methods should be considered. In particular, it is interesting to check under what conditions the rapidly varying (sine) term of the density profile becomes irrelevant (a constant) and the profile given by the slowly varying envelope.

The framework developed here can be extended to other potentials and patterns. For convenience, we have considered expansions in Bessel functions, but other complete sets could be used. For example, under certain conditions, the Fourier-Bessel expansion can be considered instead, where a complete set is defined using the orthogonal versions of the Bessel function of the first kind. Future work may consider these possible extensions.

V. ACKNOWLEDGEMENTS

We acknowledge financial support from the Portuguese Foundation for Science and Technology (FCT) under Contracts nos. UID/FIS/00618/2013 and EXCL/FIS-NAN/0083/2012. DAZ also acknowledges financial support from Russian Science Foundation (grant No. 17-11-01004).

-
- [1] M. C. Cross and P. C. Hohenberg, *Rev. Mod. Phys.* **65**, 851 (1993).
 - [2] D. Walgraef, *Spatio-temporal pattern formation: with examples from Physics, Chemistry, and Materials Science* (Springer-Verlag, New York, 1997).
 - [3] A. van Blaaderen and P. Wiltzius, *Science* **270**, 1177 (1995).
 - [4] A. van Blaaderen, *Nature* **439**, 545 (2006).
 - [5] S.-H. Kim, S. Y. Lee, and S.-M. Yang, *NPG Asia Mater* **3**, 25 (2011).
 - [6] M. H. Lash, M. V. Fedorchak, J. J. McCarthy, and S. R. Little, *Soft Matter* **11**, 5597 (2015).
 - [7] P. F. Damasceno, M. Engel, and S. C. Glotzer, *Science* **337**, 453 (2012).
 - [8] S. Sacanna, D. J. Pine, and G.-R. Yi, *Soft Matter* **9**, 8096 (2013).
 - [9] C. S. Dias, N. A. M. Araújo, and M. M. Telo da Gama, *Soft Matter* **9**, 5616 (2013).
 - [10] N. M. Silvestre, Q. Liu, B. Senyuk, I. I. Smalyukh, and M. Tasinkevych, *Phys. Rev. Lett.* **112**, 225501 (2014).
 - [11] V. Garbin, *Phys. Today* **66**, 68 (2013).
 - [12] D. Joshi, D. Bargteil, A. Caciagli, J. Burelbach, Z. Xing, A. S. Nunes, D. E. P. Pinto, N. A. M. Araújo, J. Bruijc, and E. Eiser, *Science Advances* **2**, e1600881 (2016).
 - [13] A. Cadilhe, N. A. M. Araújo, and V. Privman, *J. Phys.: Condens. Matter* **19**, 065124 (2007).
 - [14] N. A. M. Araújo, A. Cadilhe, and V. Privman, *Phys. Rev. E* **77**, 031603 (2008).
 - [15] N. A. M. Araújo, C. S. Dias, and M. M. T. da Gama, *J. Phys.: Condens. Matter* **27**, 194123 (2015).
 - [16] N. A. M. Araújo, C. S. Dias, and M. M. T. da Gama, *J. Phys.: Condens. Matter* **29**, 014001 (2017).
 - [17] M. Trau, S. Sankaran, D. A. Saville, and I. A. Aksay, *Nature* **374**, 437 (1994).
 - [18] J. S. Park and D. Saintillan, *Phys. Rev. E* **83**, 041409 (2011).
 - [19] J. W. Swan, J. L. Bauer, Y. Liu, and E. M. Furst, *Soft Matter* **10**, 1102 (2014).
 - [20] S. M. Cattes, S. H. L. Klapp, and M. Schoen, *Phys. Rev. E* **91**, 052127 (2015).
 - [21] H. Löwen, *Eur. Phys. J. Spec. Top.* **222**, 2727 (2013).
 - [22] J. Dobnikar, A. Snezhko, and A. Yethiraj, *Soft Matter* **9**, 3693 (2013).
 - [23] G. B. Davies, T. Krüger, P. V. Coveney, J. Harting, and F. Bresme, *Adv. Mater.* **26**, 6715 (2014).
 - [24] P. Dillmann, G. Maret, and P. Keim, *Eur. Phys. J. Spec. Top.* **222**, 2941 (2013).
 - [25] A. F. Demirörs, P. P. Pillai, B. Kowalczyk, and B. A. Grzybowski, *Nature* **503**, 99 (2013).
 - [26] F. Evers, R. Hanes, C. Zunke, R. Capellmann, J. Berwunge, C. Dalle-Ferrier, M. Jenkins, I. Ladadwa, A. Heuer, R. Castañeda Priego, and S. Egelhaaf, *Eur. Phys. J. Spec. Top.* **222**, 2995 (2013).
 - [27] R. M. Erb, H. S. Son, B. Samanta, V. M. Rotello, and B. B. Yellen, *Nature* **457**, 999 (2009).
 - [28] J.-B. Delfau, H. Ollivier, C. López, B. Blasius, and E. Hernández-García, *Phys. Rev. E* **94**, 042120 (2016).
 - [29] U. M. B. Marconi and P. Tarazona, *J. Chem. Phys.* **110**, 8032 (1999).
 - [30] U. M. B. Marconi and P. Tarazona, *J. Phys: Condens. Matter* **12**, A413 (2000).

- [31] M. Rauscher, *J. Phys.: Condens. Matter* **22**, 364109 (2010).
- [32] B. D. Goddard, A. Nold, N. Savva, G. A. Pavliotis, and S. Kalliadasis, *Phys. Rev. Lett.* **109**, 120603 (2012).
- [33] A. S. Nunes, N. A. M. Araújo, and M. M. Telo da Gama, *J. Chem. Phys.* **144**, 034902 (2016).